

Correlative study of flavor anomalies and dark matter in the light of scalar leptoquark

Manas Kumar Mohapatra^{a,*} Shivaramakrishna

Singirala^{a,b,†} Dhiren Panda^{a,‡} and Rukmani Mohanta^{a,§}

^a*School of Physics, University of Hyderabad, Hyderabad-500046, India*

^b*School of Physical Sciences, Indian Association for the Cultivation of Science,
2A & 2B Raja S.C Mullick Road, Kolkata-700032, India (current affiliation)*

Abstract

We explore $U(1)_{L_e-L_\mu}$ gauge extension of the Standard Model with particle content enlarged by three neutral fermions, of which the lightest one contributes to dark matter content of the Universe. The scalar sector is enriched with a \tilde{R}_2 scalar leptoquark doublet to investigate flavor anomalies in B -meson sector, an additional inert scalar doublet to realize neutrino mass at one loop and a scalar singlet to spontaneously break the new $U(1)$. We discuss dark matter relic density and direct detection cross section in scalar and gauge portals. New physics contribution for $b \rightarrow s$ transition comes from penguin diagrams with Z' , leptoquark and new fermions. We analyze the constraints on the model parameters from the established observables of $B \rightarrow K^{(*)}\mu^+\mu^-$ and $B_s \rightarrow \phi\mu^+\mu^-$ decay channels. Utilizing the permissible parameter space consistent with both flavor and dark sectors, we discuss the impact on various observables such as branching ratio, forward-backward asymmetry, longitudinal polarisation asymmetry, and also lepton non-universality of $\Lambda_b \rightarrow \Lambda^*(1520)(\rightarrow pK)\ell^+\ell^-$ decay channel.

*Electronic address: manasmohapatra12@gmail.com

†Electronic address: krishnas542@gmail.com

‡Electronic address: pandadhiren530@gmail.com

§Electronic address: rmisp@uohyd.ernet.in

I. INTRODUCTION

The Standard Model (SM) of particle physics has been extremely triumphant in explaining the physics at elementary level. However, it fails to provide suitable explanation for several aspects. Listing a few, the nature and existence of dark matter (DM) [1–6], light neutrino masses and its oscillation phenomena [7], matter-antimatter asymmetry of the Universe [8–12] etc and anomalies associated with the B -meson sector.

Flavor-changing neutral current (FCNC) processes are important probes for physics beyond the SM. In particular, the $b \rightarrow s\mu^+\mu^-$ transition has recently attracted considerable interest due to anomalies detected in LHCb and Belle II experiments. The most compelling observables in $b \rightarrow s\ell\ell$ transitions, which have garnered significant attention for providing clear indications of new physics (NP), are the ratios R_K and R_{K^*} [13], defined as

$$R_{K^{(*)}} = \frac{\mathcal{B}(B \rightarrow K^{(*)}\mu\mu)}{\mathcal{B}(B \rightarrow K^{(*)}ee)}, \quad (1)$$

which are predicted to be 1 in the SM, representing lepton flavor universality (LFU). They are theoretically clean as hadronic uncertainties cancel out in these ratios. Recent updates from LHCb [14, 15] have confirmed that the measured values of these observables align with their SM predictions. Nevertheless, a range of other observables in $b \rightarrow s\ell\ell$ transitions, such as the notable P'_5 observable and various branching fractions, exhibit deviations of several sigma from SM predictions. Specifically, the LHCb [16, 17] and ATLAS [18] collaborations report a 3.3σ deviation in the measurement of P'_5 from the SM expectation. Additionally, the branching ratio for the $B_s \rightarrow \phi\mu^-\mu^+$ decay shows a 3.3σ deviation [19, 20] in the q^2 range of $[1.1, 6.0]$ GeV^2 . Furthermore, the measurements of $R_{K_S^0}$ and $R_{K^{*+}}$ [21] also exhibit deviations from their SM predictions of 1.4σ and 1.5σ , respectively. Similarly, various other observables such as forward-backward asymmetries, longitudinal polarization asymmetries, CP-averaged observables, CP asymmetries in $B \rightarrow K^{(*)}\mu^+\mu^-$ decay processes across multiple q^2 intervals indicate few sigma deviations from their SM expectations. Consequently, the observations do not entirely exclude the possibility of new physics in FCNC-mediated $b \rightarrow s\ell\ell$ transitions. Various analyses, both model-dependent and model-independent, have been performed to account for $b \rightarrow s\ell^+\ell^-$ transition decays [22–48].

To confirm these hints of NP in $b \rightarrow s\ell^+\ell^-$, it is crucial to exploit the growing dataset from the LHCb experiment, not only for more precise measurements of known observables but

also to explore other decays probing the same underlying physics. In this regard, motivated by the observed discrepancies between the measured values and SM predictions in the above discussed transitions, we exploit the decay of the Λ_b baryon into excited Λ state through the decay channel $\Lambda_b \rightarrow (\Lambda^*(1520) \rightarrow pK)\ell^+\ell^-$. This channel offers valuable insights into the dynamics of flavor transitions, shedding light on the underlying processes and enhancing our understanding of the implications of potential new physics. Among the semileptonic decay modes of Λ_b to hadrons, the decay to the $\Lambda^*(1520)$ is particularly noteworthy due to its narrow width and its significance in pentaquark searches by the LHCb collaboration through the decay $\Lambda_b^0 \rightarrow pKJ/\psi$ [49]. In addition, the Λ^* , characterized by its $J^P = 3/2^-$ spin-parity and its strong decay into the $p\bar{K}$ pair, stands out from neighboring states such as the $\Lambda(1600)$, $\Lambda(1405)$, and the weakly decaying $\Lambda(1116)$, all of which have $J^P = 1/2^\pm$. Moreover, this mode has garnered significant attention for its distinct theoretical environment, even though it has not been observed experimentally. A recent measurement from LHCb experiment [50] presents the first test of lepton universality in the baryon sector, achieved by measuring the ratio of branching fractions for the decays $\Lambda_b^0 \rightarrow pK^-\mu^+\mu^-$ and $\Lambda_b^0 \rightarrow pK^-e^+e^-$, referred to as R_{pK} . While the ratio R_{pK} is compatible with SM predictions, there is a noticeable suppression in $\mathcal{B}(\Lambda_b \rightarrow pK\mu\bar{\mu})$ relative to $\mathcal{B}(\Lambda_b \rightarrow pKe\bar{e})$. Therefore, interpreting this findings requires precise theoretical knowledge of the various excited Λ states contributing to the broad pK region, highlighting the necessity of developing a comprehensive understanding of these excited states. Taking this into account, it is quite intriguing to investigate the decay channel $\Lambda_b \rightarrow \Lambda^*(1520)(\rightarrow pK)\ell\ell$ within the Standard Model and beyond.

The aim of this paper is to address flavor anomalies by realizing a new diagram for $b \rightarrow s$ transition via a scalar leptoquark and a weakly interacting massive particle (WIMP) dark matter. By extending SM gauge symmetry with an additional $U(1)$, we obtain new physics contribution in B -meson sector via Z' . The new gauge parameters and the new Yukawa dictate the new physics contribution. Moreover, the scalar leptoquark and Z' can also mediate in DM annihilations to meet the dark matter budget of the Universe and also provide spin-dependent WIMP-nucleon cross section. In this work, we propose a new physics model based on a local $U(1)_{L_e-L_\mu}$ gauge extension of the SM to address the $b \rightarrow s\mu^+\mu^-$ anomaly.

This paper is structured as follows: Section II introduces the model, detailing the particle content, relevant interaction Lagrangian terms, mixing matrices, and their diagonalization.

Section III discusses the relic density of fermionic dark matter and the direct detection cross section. A brief discussion on light neutrino masses is presented in Section IV. In Section V and VI, we constrain the new physics parameter space from the flavor sector and explore the implications of new physics on the decay channel $\Lambda_b \rightarrow \Lambda^*(1520)(\rightarrow pK)\ell\ell$, respectively. Finally, our conclusions are summarized in Section VII.

II. NEW MODEL WITH LEPTOQUARKS

We consider a variant of $L_e - L_\mu$ model to address anomalies associated with B meson, dark matter and light neutrino mass. To obtain a suitable platform for a correlative study, we enrich the model with three neutral fermions N_e, N_μ, N_τ , a scalar leptoquark \tilde{R}_2 and an inert scalar doublet (η). Alongside, a singlet ϕ_2 is included to spontaneously break the new $U(1)$ gauge symmetry. Similar works in the context of $L_\mu - L_\tau$ gauge extension can be looked at in [22, 23]. The full list of field content is provided in Table. I. The relevant

	Field	$SU(3)_C \times SU(2)_L \times U(1)_Y$	$U(1)_{L_e-L_\mu}$	Z_2
Fermions	$Q_L \equiv (u, d)_L^T$	$(\mathbf{3}, \mathbf{2}, 1/6)$	0	+
	u_R	$(\mathbf{3}, \mathbf{1}, 2/3)$	0	+
	d_R	$(\mathbf{3}, \mathbf{1}, -1/3)$	0	+
	$\ell_{\alpha L} \equiv (\nu_\alpha, \alpha)_L, \alpha = e, \mu, \tau$	$(\mathbf{1}, \mathbf{2}, -1/2)$	1, -1, 0	+
	$\ell_R \equiv \alpha_R, \alpha = e, \mu, \tau$	$(\mathbf{1}, \mathbf{1}, -1)$	1, -1, 0	+
	N_e, N_μ, N_τ	$(\mathbf{1}, \mathbf{1}, 0)$	1, -1, 0	-
Scalars	H	$(\mathbf{1}, \mathbf{2}, 1/2)$	0	+
	η	$(\mathbf{1}, \mathbf{2}, 1/2)$	0	-
	ϕ_2	$(\mathbf{1}, \mathbf{1}, 0)$	2	+
	\tilde{R}_2	$(\mathbf{3}, \mathbf{2}, 1/6)$	1	-

TABLE I: Fields in the chosen $U(1)_{L_e-L_\mu}$ model.

Lagrangian terms corresponding to gauge, fermion, gauge-fermion interaction and scalar

sectors are given by

$$\begin{aligned}
\mathcal{L} = & \mathcal{L}_{\text{SM}} - \frac{1}{4} Z'_{\mu\nu} Z'^{\mu\nu} - g_{e\mu} \bar{\ell}_e \gamma^\mu \ell_e Z'_\mu - g_{e\mu} \bar{e}_R \gamma^\mu e_R Z'_\mu + g_{e\mu} \bar{\ell}_{\mu L} \gamma^\mu \ell_{\mu L} Z'_\mu + g_{e\mu} \bar{\mu}_R \gamma^\mu \mu_R Z'_\mu \\
& + \bar{N}_e (i\not{\partial} - g_{e\mu} Z'_\mu \gamma^\mu) N_e + \bar{N}_\mu (i\not{\partial} + g_{e\mu} Z'_\mu \gamma^\mu) N_\mu + \bar{N}_\tau i\not{\partial} N_\tau - \frac{f_e}{2} (\bar{N}_e^c N_e \phi_2^\dagger + \text{h.c.}) \\
& - \frac{f_\mu}{2} (\bar{N}_\mu^c N_\mu \phi_2 + \text{h.c.}) - \frac{1}{2} M_{\tau\tau} \bar{N}_\tau^c N_\tau - M_{e\mu} (\bar{N}_e^c N_\mu + \bar{N}_\mu^c N_e) - \sum_{\alpha, \beta=e, \mu, \tau} (Y_{\alpha\beta} \bar{\ell}_{L\alpha} \tilde{\eta} N_{\beta R} + \text{h.c.}) \\
& - (y_{qRN} \bar{Q}_L \tilde{R}_2 N_{\mu R} + \text{h.c.}) + \left| \left(i\partial_\mu - \frac{g}{2} \boldsymbol{\tau}^a \cdot \mathbf{W}_\mu^a - \frac{g'}{6} B_\mu + g_{e\mu} Z'_\mu \right) \tilde{R}_2 \right|^2 + |(i\partial_\mu - 2g_{e\mu} Z'_\mu) \phi_2|^2 \\
& + \left| \left(i\partial_\mu - \frac{g}{2} \boldsymbol{\tau}^a \cdot \mathbf{W}_\mu^a - \frac{g'}{2} B_\mu \right) \eta \right|^2 - V(H, \tilde{R}_2, \eta, \phi_2), \tag{2}
\end{aligned}$$

where, the scalar potential is expressed as

$$\begin{aligned}
V(H, \tilde{R}_2, \eta, \phi_2) = & \mu_H^2 (H^\dagger H) + \lambda_H (H^\dagger H)^2 + \mu_\eta^2 (\eta^\dagger \eta) + \lambda_{H\eta} (H^\dagger H) (\eta^\dagger \eta) + \lambda_\eta (\eta^\dagger \eta)^2 + \lambda'_{H\eta} (H^\dagger \eta) (\eta^\dagger H) \\
& + \frac{\lambda''_{H\eta}}{2} [(H^\dagger \eta)^2 + \text{h.c.}] + \mu_\phi^2 (\phi_2^\dagger \phi_2) + \lambda_\phi (\phi_2^\dagger \phi_2)^2 + \mu_R^2 (\tilde{R}_2^\dagger \tilde{R}_2) + \lambda_R (\tilde{R}_2^\dagger \tilde{R}_2)^2 \\
& + \lambda_{H\phi} (\phi_2^\dagger \phi_2) (H^\dagger H) + \lambda_{R\phi} (\phi_2^\dagger \phi_2) (\tilde{R}_2^\dagger \tilde{R}_2) + \lambda_{\eta\phi} (\phi_2^\dagger \phi_2) (\eta^\dagger \eta) + \lambda_{R\eta} (\tilde{R}_2^\dagger \tilde{R}_2) (\eta^\dagger \eta) \\
& + \lambda_{HR} (H^\dagger H) (\tilde{R}_2^\dagger \tilde{R}_2) + \lambda'_{HR} (H^\dagger \tilde{R}_2) (\tilde{R}_2^\dagger H). \tag{3}
\end{aligned}$$

In the above, the new scalar doublets are denoted by \tilde{R}_2 and η are given by $\eta = \begin{pmatrix} \eta^+ \\ \eta^0 \end{pmatrix}$,

with $\eta^0 = \frac{\eta_R + i\eta_I}{\sqrt{2}}$ and $\tilde{R}_2 = \begin{pmatrix} \tilde{R}_2^{2/3} \\ \tilde{R}_2^{-1/3} \end{pmatrix}$. After spontaneous symmetry breaking the masses of scalars are denoted by

$$\begin{aligned}
M_C^2 &= \mu_\eta^2 + \frac{\lambda_{H\eta}}{2} v^2 + \frac{\lambda_{\eta\phi}}{2} v_2^2, \\
M_R^2 &= \mu_\eta^2 + (\lambda_{H\eta} + \lambda'_{H\eta} + \lambda''_{H\eta}) \frac{v^2}{2} + \frac{\lambda_{\eta\phi}}{2} v_2^2, \\
M_I^2 &= \mu_\eta^2 + (\lambda_{H\eta} + \lambda'_{H\eta} - \lambda''_{H\eta}) \frac{v^2}{2} + \frac{\lambda_{\eta\phi}}{2} v_2^2, \\
M_U^2 &= \mu_R^2 + \frac{\lambda_{HR}}{2} v^2 + \frac{\lambda_{R\phi}}{2} v_2^2, \\
M_D^2 &= \mu_R^2 + (\lambda_{HR} + \lambda'_{HR}) \frac{v^2}{2} + \frac{\lambda_{R\phi}}{2} v_2^2. \tag{4}
\end{aligned}$$

In the above M_C, M_R, M_I represent the masses of charged and neutral constituents of inert doublet, M_U, M_D correspond to the masses of leptoquark components $\tilde{R}_2^{2/3}, \tilde{R}_2^{-1/3}$ respectively. Furthermore, the mass of associated gauge boson of new $U(1)$ is $M_{Z'} = 2v_2 g_{e\mu}$.

A. Fermion and scalar spectrum

The fermion and scalar mass matrices take the form

$$M_N = \begin{pmatrix} \frac{1}{\sqrt{2}}f_e v_2 & M_{e\mu} \\ M_{e\mu} & \frac{1}{\sqrt{2}}f_\mu v_2 \end{pmatrix}, \quad M_S = \begin{pmatrix} 2\lambda_H v^2 & \lambda_{H2} v v_2 \\ \lambda_{H2} v v_2 & 2\lambda_2 v_2^2 \end{pmatrix}. \quad (5)$$

One can diagonalize the above mass matrices by $U_{\delta(\zeta)}^T M_{N(S)} U_{\delta(\zeta)} = \text{diag} [M_{N1(H1)}, M_{N2(H2)}]$, where

$$U_\theta = \begin{pmatrix} \cos \theta & \sin \theta \\ -\sin \theta & \cos \theta \end{pmatrix}, \quad (6)$$

with $\zeta = \frac{1}{2} \tan^{-1} \left(\frac{\lambda_{H2} v v_2}{\lambda_2 v_2^2 - \lambda_H v^2} \right)$ and $\delta = \frac{1}{2} \tan^{-1} \left(\frac{2M_{e\mu}}{(f_\mu - f_e)(v_2/\sqrt{2})} \right)$.

We denote the scalar mass eigenstates as H_1 and H_2 , with H_1 is assumed to be observed Higgs at LHC with $M_{H_1} = 125.09$ GeV and $v = 246$ GeV. The mixing parameter ζ is taken minimal to stay with LHC limits on Higgs decay width. We indicate N_1 and N_2 to be the fermion mass eigenstates, with the lightest one (N_1) as the probable dark matter candidate in the present work.

III. DARK MATTER PHENOMENOLOGY

A. Relic density

The model provides fermionic dark matter candidate N_1 , with mass ranging up to 1 TeV range. The DM fermion can couple to LQ components $\tilde{R}_2^{-1/3}$ and can annihilate to $q''\bar{q}'''$ with $q'', q''' = d, s, b$. Further, it can couple to $\tilde{R}_2^{2/3}$ and annihilate to $q\bar{q}'$ with $q, q' = u, c, t$ in final state. In gauge portal, the DM can couple to Z' and can lead to s-channel annihilations with $e\bar{e}$, $\nu_e\bar{\nu}_e$, $\mu\bar{\mu}$, $\nu_\mu\bar{\nu}_\mu$ as final state particles. The corresponding Feynman diagrams are provided in the upper panel of Fig. 1. Inert scalar masses are large, hence annihilations of dark matter via η gets suppressed. The abundance of dark matter can be computed by

$$\Omega h^2 = \frac{1.07 \times 10^9 \text{ GeV}^{-1}}{M_{\text{Pl}} g_*^{1/2}} \frac{1}{J(x_f)}, \quad (7)$$

where, $M_{\text{Pl}} = 1.22 \times 10^{19}$ GeV and $g_* = 106.75$ denote the Planck mass and total number of effective relativistic degrees of freedom respectively. The function J is

$$J(x_f) = \int_{x_f}^{\infty} \frac{\langle \sigma v \rangle(x)}{x^2} dx. \quad (8)$$

In the above, the thermally averaged cross section $\langle \sigma v \rangle$ reads as

$$\langle \sigma v \rangle(x) = \frac{x}{8M_{N1}^5 K_2^2(x)} \int_{4M_{N1}^2}^{\infty} \hat{\sigma} \times (s - 4M_{N1}^2) \sqrt{s} K_1 \left(\frac{x\sqrt{s}}{M_{N1}} \right) ds. \quad (9)$$

Here K_1 , K_2 are the modified Bessel functions, $x = M_{N1}/T$, with T being the temperature, M_{N1} is dark matter mass, $\hat{\sigma}$ is the dark matter cross section and x_f stands for the freeze-out parameter.

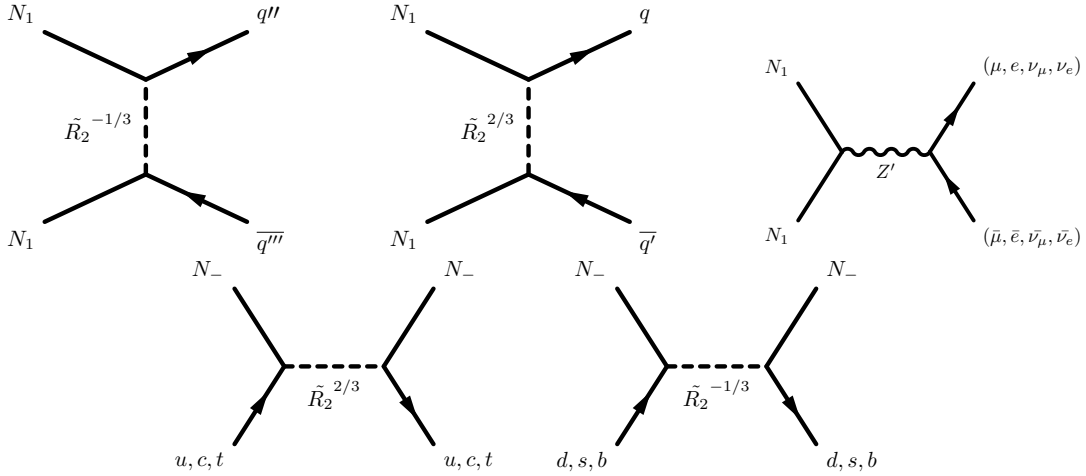


FIG. 1: Feynman diagrams contributing to relic density and WIMP-nucleon cross section.

B. Direct searches

Moving to direct searches, the Z' does not directly couple to quarks, hence DM-nucleon cross section will not exist in gauge portal. However, the DM can couple to LQ components, will provide spin-dependent (SD) DM-nucleon cross section, whose sensitivity can be checked with stringent upper bound of PICO experiment. The Feynman diagrams are provided in the lower panel of Fig. 1 and the effective interaction Lagrangian takes the form

$$\mathcal{L}_{\text{eff}} \simeq \frac{y_{qRN}^2 \sin^2 \delta}{4M_{\text{LQ}}^2} \bar{N}_1 \gamma^\mu \gamma^5 N_1 \bar{q} \gamma_\mu \gamma^5 q. \quad (10)$$

The spin-dependent cross section takes the form [51]

$$\sigma_{\text{SD}} = \frac{\mu_r^2 \sin^4 \delta}{\pi M_{\text{LQ}}^4} y_{qRN}^4 [\Delta_d + \Delta_d + \Delta_s]^2 J_n(J_n + 1), \quad (11)$$

where, $M_{\text{LQ}} = M_U$ and M_D for up-type and down-type quarks respectively, angular momentum $J_n = \frac{1}{2}$, reduced mass being $\mu_r = \frac{M_{N1} M_n}{M_{N1} + M_n}$ with $M_n \simeq 1$ GeV for nucleon. Values of quark spin functions Δ_q are given in [51]. We have implemented the model in LanHEP [52] package and used micrOMEGAs [53–55] to compute relic density and also DM-nucleon cross section. Spin-independent DM-nucleon cross section in Higgs portal does not provide any new constraints on the model parameter space. The cross section can be brought down by choosing small scalar mixing angle (i.e., ζ).

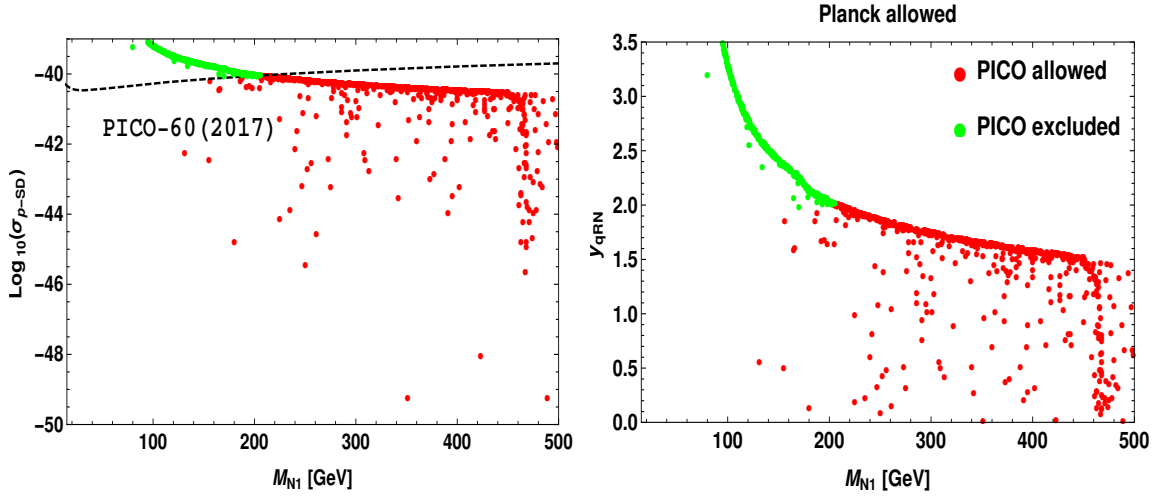


FIG. 2: WIMP-nucleon cross section as a function of dark matter mass projected in the left panel. Dashed line corresponds to PICO-60 limit [56]. Right panel displays the favourable region in the plane of $y_{qRN} - M_{N1}$ plane showing same color contrast as the left panel.

C. Analysis

Left panel of Fig. 2 projects the SD DM-proton cross section as a function of DM mass. The green data points seem to violate the stringent PICO [56] limit. Right panel shows that the Yukawa is indeed constrained by color contrast. First dip is due to s-channel resonance in Z' propagator with mass $M_{Z'} = 671$ GeV. Second dip is due to resonance in H_2 propagator i.e., $M_{H_2} = 800$ GeV. A small dip around 60 GeV is because of resonance in H_1 propagator.

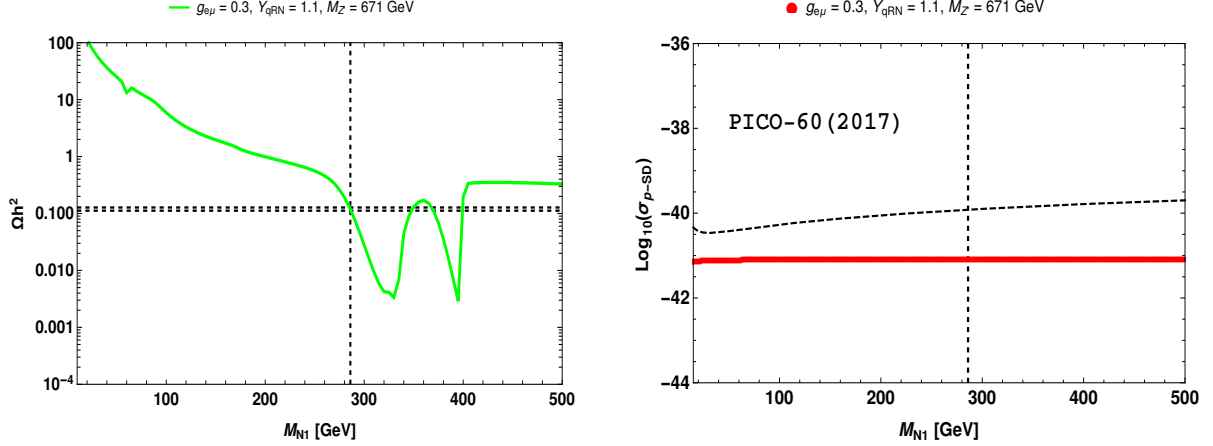


FIG. 3: Left panel projects relic density as a function of dark matter mass with horizontal dashed lines correspond to Planck 3σ constraint on relic density [57]. Right panel depicts spin-dependent DM-nucleon cross section with upper limit representing PICO-60 [56]. The input parameters are provided in Table. III.

Left panel of Fig. 3 projects DM relic density meeting Planck satellite data [57] for a 286 GeV dark matter and other parameter values are provided in Table. III. Right panel displays SD DM-proton cross section for the same 286 GeV dark matter and of the benchmark provided in Table. III.

IV. COMMENTS ON NEUTRINO MASS

Neutrino mass can be generated at one-loop from the Yukawa interaction with the inert doublet η . Assuming $(M_R^2 + M_I^2)/2 = m_0^2$ is very much greater than $M_R^2 - M_I^2 = \lambda_{H\eta}'' v^2$, the expression for the one-loop neutrino mass [58, 59] takes the form

$$(\mathcal{M}_\nu)_{\beta\gamma} = \frac{\lambda_{H\eta}'' v^2}{32\pi^2} \sum_{i=1}^3 \frac{Y_{\beta i} Y_{\gamma i}}{M_{ii}} \left[\frac{M_{ii}^2}{m_0^2 - M_{ii}^2} + \frac{M_{ii}^4}{(m_0^2 - M_{ii}^2)^2} \ln \frac{M_{ii}^2}{m_0^2} \right], \quad (12)$$

where $M_{ij} = \text{diag}(M_{N1}, M_{N2}, M_{\tau\tau})$. For $m_0 \sim 5$ TeV, $\lambda_5 \sim 10^{-2}$ and $Y \sim 10^{-2}$, one can obtain neutrino mass at sub-eV scale. It should be noted that the $L_e - L_\mu$ charges of heavy fermions and SM leptons are same for each generation while the inert doublet is assigned with charge zero, the Yukawa matrix Y is diagonal. Therefore, the neutrino mass matrix (12) is diagonal by model construction.

V. CONSTRAINTS ON NEW PHYSICS FROM THE FLAVOR SECTOR

The most general effective Hamiltonian mediating the $b \rightarrow sl^+l^-$ transition is given by [32, 60]

$$\mathcal{H}_{\text{eff}} = -\frac{4G_F}{\sqrt{2}}V_{tb}V_{ts}^* \left[\sum_{i=1}^6 C_i(\mu)O_i + \sum_{i=9,10} \left(C_i(\mu)O_i + C'_i(\mu)O'_i \right) \right], \quad (13)$$

where G_F is the Fermi constant, $V_{tb}V_{ts}^*$ denote the CKM matrix elements, C_i 's stand for the Wilson coefficients evaluated at the renormalized scale $\mu = m_b$ [61].

Here O_i 's represent dimension-six operators responsible for leptonic/semileptonic processes, given as

$$O_9^{(\prime)} = \frac{\alpha_{\text{em}}}{4\pi} (\bar{s}\gamma^\mu P_{L(R)}b)(\bar{l}\gamma_\mu l), \quad O_{10}^{(\prime)} = \frac{\alpha_{\text{em}}}{4\pi} (\bar{s}\gamma^\mu P_{L(R)}b)(\bar{l}\gamma_\mu \gamma_5 l), \quad (14)$$

where, α_{em} is the fine-structure constant, $P_{L,R} = (1 \mp \gamma_5)/2$ are the chiral operators.

The one-loop diagrams contributing non-zero values to the rare $b \rightarrow sll$ processes can arise through the exchange of $Z', H_{1,2}$ particles, forming penguin diagrams with the scalar leptoquark $\tilde{R}_2^{-1/3}$ and $N_{1,2}$ particles within the loop, as depicted in Fig. 4. In the present framework, the one-loop penguin diagram illustrated in the top-left panel significantly contributes to the process. However, the diagram corresponding to the right panel yields negligible contribution to the $b \rightarrow s\ell\ell$ transition as it is suppressed by $m_b/M_{N_{1,2}}$. The loop functions of the lower two diagrams are suppressed by the factor $m_q M_{N_{1,2}}/M_{\tilde{R}_2}^2$ ($q = b, s$) resulting in minimal contribution to $b \rightarrow sll$ processes. Thus, only the top-left diagram, mediated via Z' boson, substantially contributes to the $b \rightarrow s\ell\ell$ channels.

In the presence of Z' exchanging one loop diagram, the transition amplitude of semileptonic $b \rightarrow sll$ decay process is given as

$$\mathcal{M} = -\frac{1}{(4\pi)^2} \frac{y_{qRN}^2 g_{e\mu}^2 (\text{Sin}2\delta)^2}{4} \frac{\mathcal{R}(a, b)}{m_{Z'}^2} [\bar{s}(p')\gamma^\mu P_L b(p)][\bar{\mu}(q_2)\gamma_\mu \mu(q_1)], \quad (15)$$

which in comparison with the generalized effective Hamiltonian provides additional new Wilson coefficient as

$$C_9^{\text{NP}} = -\frac{1}{4\pi} \frac{\sqrt{2}}{4G_F m_{Z'}^2} \frac{1}{\alpha_{em}} \frac{y_{qRN}^2 g_{e\mu}^2}{V_{tb}V_{ts}^*} \mathcal{R}(a, b), \quad (16)$$

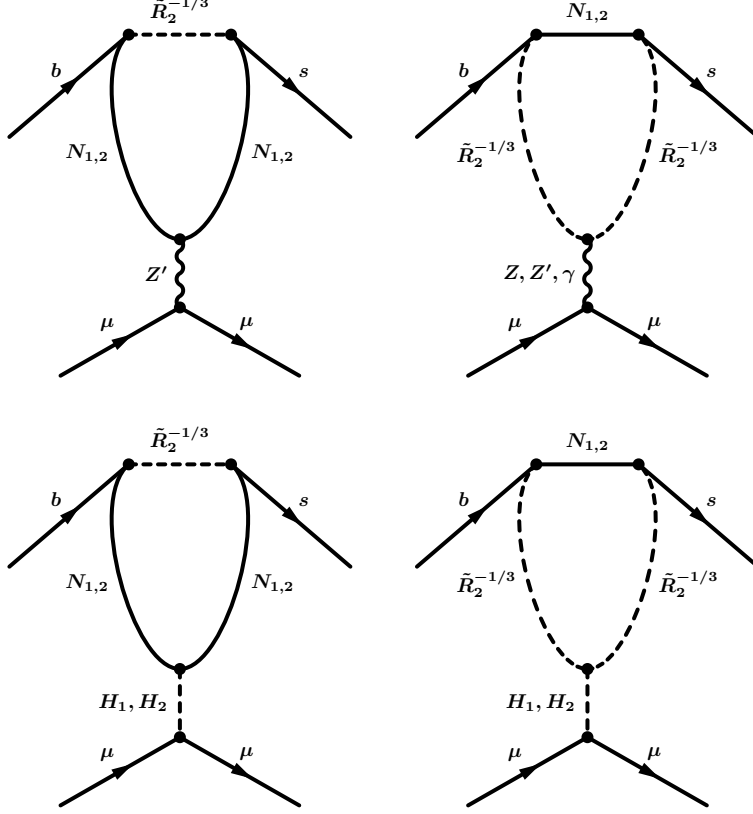


FIG. 4: Allowed penguin diagrams illustrating the $b \rightarrow s\mu\mu$ transition in the model.

where the loop function is given as

$$\mathcal{R}(a, b) = \left[\frac{3}{2} \left\{ \left(\frac{1}{2} - \frac{\sqrt{a}\sqrt{b}}{a-b} \left(\frac{a \log a}{a-1} - \frac{b \log b}{b-1} \right) - \frac{1}{2(a-b)} \left(\frac{a^2 \log a}{a-1} - \frac{b^2 \log b}{b-1} \right) \right\} \right. \\ \left. - \frac{3}{2} \left(\frac{1}{8} - \frac{3-3b^2+8b \log b-2b^2 \log b}{8(b-1)^2} \right) + \frac{1}{2} \left(\frac{1}{8} - \frac{3-3a^2+8a \log a-2a^2 \log a}{8(a-1)^2} \right) \right] \quad (17)$$

with $a = \frac{m_{N_1}^2}{m_{LQ}^2}$ and $b = \frac{m_{N_2}^2}{m_{LQ}^2}$.

Our goal is to constrain the model parameters related to the leptoquark (LQ) and Z' couplings by analyzing decay modes involving $b \rightarrow s\mu^+\mu^-$ transitions, specifically $B \rightarrow K\mu^+\mu^-$, $B \rightarrow K^*\mu^+\mu^-$, and $B_s \rightarrow \phi\mu^+\mu^-$ processes. We investigate the branching ratios for $B^0 \rightarrow K^{*0}\mu^+\mu^-$, $B^+ \rightarrow K^{*+}\mu^+\mu^-$, $B^0 \rightarrow K^0\mu^+\mu^-$, and $B^+ \rightarrow K^+\mu^+\mu^-$ [62, 63], across various q^2 bins. Additionally, our analysis incorporates the updated branching fractions for $B_s \rightarrow \phi\mu^+\mu^-$ as measured by LHCb over different q^2 intervals [19]. We also include measurements of the forward-backward asymmetry (A_{FB}) [17], longitudinal polarization frac-

tion (F_L), CP-averaged observables ($S_{i=3,4,5,7,8,9}$), CP asymmetries ($A_{i=3,4,5,7,8,9}$), and form factor-independent observables ($P_1 - P'_8$) [64] across multiple q^2 intervals such as $[0.10, 0.98]$, $[1.1, 2.5]$, $[2.5, 4.0]$, $[4.0, 6.0]$, and $[1.1, 6.0]$.

In addition to the optimized observables ($P_1 - P'_8$), LHCb has provided an extensive set of angular observables for these decay modes across various q^2 intervals [65]. Our analysis also focuses on exploring the NP coupling C_9^{NP} within the muon sector. For this study, we utilize all the discussed observables and carry out our analysis utilizing the *flavio* package [66]. The allowed parameter space is depicted in Fig. 5. In this analysis, we consider the benchmark values of the parameters as shown in Table III.

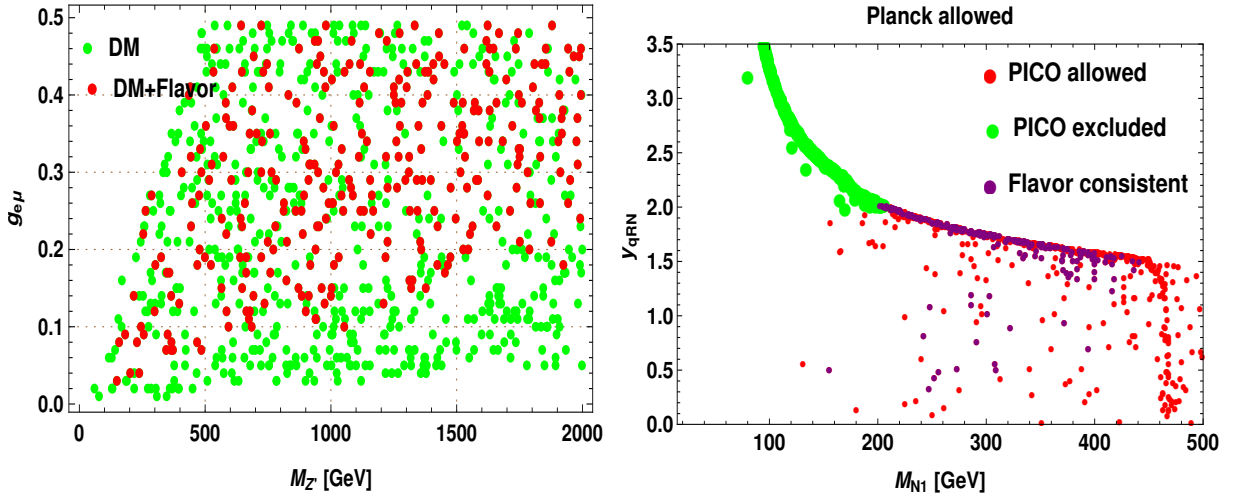


FIG. 5: Allowed parameter space illustrating the $b \rightarrow s\mu\mu$ transition in this model.

TABLE II: Values of the input parameters [67] used in our analysis.

Parameter	Value	Parameter	Value	Parameter	Value
G_F	$1.166 \times 10^{-5} \text{ GeV}^{-2}$	m_u	0.003 GeV	m_{Λ_b}	5.619 GeV
τ_{Λ_b}	$(1.470 \pm 0.010) \times 10^{-12} \text{ s}$	m_c	1.270 GeV	m_{Λ^*}	1.519 GeV
$ V_{tb}V_{ts}^* $	0.0401 ± 0.001	m_b	4.18 GeV	m_μ	0.105 GeV
α_e	1/127.925	\mathcal{B}_{Λ^*}	0.45 ± 0.01	m_e	0.0005 GeV

Parameter	y_{qRN}	$g_{e\mu}$	$M_{Z'}$ [GeV]	M_{N1} [GeV]
Bechmark	1.1	0.3	671	286

TABLE III: Sample benchmark values chosen from the allowed paramter space of Fig. 5.

VI. INSPECTION OF NEW PHYSICS IN $\Lambda \rightarrow \Lambda^*(1520)(\rightarrow pK^-)\ell^+\ell^-$ DECAYS

Having established the benchmark values for the new vector coefficient, we proceed to examine their effects on the decay observables of the exclusive $\Lambda \rightarrow \Lambda^*(1520)(\rightarrow pK^-)\ell^+\ell^-$ channel. This analysis aims to elucidate the impact of new physics parameters associated with the coupling C_9^{NP} on the decay dynamics, thereby providing a deeper understanding of how new physics might influence this process.

A. Decay observables of $\Lambda \rightarrow \Lambda^*(1520)(\rightarrow pK^-)\ell^+\ell^-$ process

The four-fold angular distribution for the exclusive $\Lambda \rightarrow \Lambda^*(\rightarrow pK^-)\ell^+\ell^-$ decay mode can be expressed as [68, 69]

$$\begin{aligned} \frac{d^4\mathcal{B}}{dq^2 d\cos\theta_\ell d\cos\theta_{\Lambda^*} d\phi} = \frac{3}{8\pi} & \left[\left(\mathcal{K}_{1c} \cos\theta_\ell + \mathcal{K}_{1cc} \cos^2\theta_\ell + \mathcal{K}_{1ss} \sin^2\theta_\ell \right) \cos^2\theta_{\Lambda^*} \right. \\ & + \left(\mathcal{K}_{2c} \cos\theta_\ell + \mathcal{K}_{2cc} \cos^2\theta_\ell + \mathcal{K}_{2ss} \sin^2\theta_\ell \right) \sin^2\theta_{\Lambda^*} \\ & + \left(\mathcal{K}_{3ss} \sin^2\theta_\ell \right) \sin^2\theta_{\Lambda^*} \cos\phi + \left(\mathcal{K}_{4ss} \sin^2\theta_\ell \right) \sin^2\theta_{\Lambda^*} \sin\phi \cos\phi \\ & + \left(\mathcal{K}_{5s} \sin\theta_\ell + \mathcal{K}_{5sc} \sin\theta_\ell \cos\theta_\ell \right) \sin\theta_{\Lambda^*} \cos\theta_{\Lambda^*} \cos\phi \\ & \left. + \left(\mathcal{K}_{6s} \sin\theta_\ell + \mathcal{K}_{6sc} \sin\theta_\ell \cos\theta_\ell \right) \sin\theta_{\Lambda^*} \cos\theta_{\Lambda^*} \sin\phi \right]. \end{aligned} \quad (18)$$

where θ_{Λ^*} represents the angle formed by the proton with the daughter baryon Λ^* in the rest frame of Λ_b . Similarly, in the rest frame of the lepton pair, θ_ℓ denotes the angle formed by the ℓ^- with respect to the direction of the daughter baryon Λ^* . Moreover, in the rest frame of Λ_b , ϕ defines the angle between the planes containing pK^- and the lepton pair. The angular coefficients $\mathcal{K}_{1c,\dots,6sc}$, can be expressed as

$$\mathcal{K}_{1c,\dots,6sc} = K_{1c,\dots,6sc} + \frac{m_\ell}{\sqrt{q^2}} K'_{1c,\dots,6sc} + \frac{m_\ell^2}{q^2} K''_{1c,\dots,6sc}. \quad (19)$$

Here the first term K corresponds to massless leptons, whereas, K' and K'' correspond to linear ($\mathcal{O}(m_\ell/\sqrt{q^2})$) and quadratic ($\mathcal{O}(m_\ell^2/q^2)$) mass corrections, respectively. The explicit expressions for $K_{\{\dots\}}$, $K'_{\{\dots\}}$ and $K''_{\{\dots\}}$ in terms of transversely amplitude are taken Ref [69].

From the differential decay distributions, one can construct several physical observables. The differential branching ratio, the lepton forward-backward asymmetry, the fraction of longitudinal polarization and the ratio of branching fraction. These are given as follows

- The differential branching ratio:

$$\frac{d\mathcal{B}}{dq^2} = \frac{1}{3} \left[K_{1cc} + 2K_{1ss} + 2K_{2cc} + 4K_{2ss} + 2K_{3ss} \right] \quad (20)$$

- The lepton polarization asymmetry:

$$F_L(q^2) = 1 - \frac{2(K_{1cc} + 2K_{2cc})}{K_{1cc} + 2(K_{1ss} + K_{2cc} + 2K_{2ss} + K_{3ss})} \quad (21)$$

- The forward-backward asymmetry:

$$A_{\text{FB}}^\ell(q^2) = \frac{3(K_{1c} + 2K_{2c})}{2[K_{1cc} + 2(K_{1ss} + K_{2cc} + 2K_{2ss} + K_{3ss})]} \quad (22)$$

- The lepton flavor universality violation observable:

$$R_{\Lambda^*}(q^2) = \frac{d\mathcal{B}/dq^2|_\mu}{d\mathcal{B}/dq^2|_e} \quad (23)$$

Using the input parameters from the PDG [67] and the light-front quark model form factor for the $\Lambda \rightarrow \Lambda^*$ transition as described in [70], we investigate the observables associated with the $\Lambda \rightarrow \Lambda^*(1520)(\rightarrow pK^-)\ell^+\ell^-$ decay channel. We provide a detailed analysis and interpretation of our results below.

B. Analysis of Results and Interpretations

In this subsection, we conduct an in-depth analysis of the $\Lambda \rightarrow \Lambda^*(1520)(\rightarrow pK^-)\ell^+\ell^-$ decay process in the presence of new physics. With all the input parameters that are pertinent to our analysis, we display the variations of all the observables w.r.t q^2 in Fig. 6. Similarly, we show the corresponding q^2 bin wise plots where we choose different bin sizes such as [0.1, 0.98], [1.1, 2.5], [2.5, 4] and [4.0, 6.0] (in the units of GeV^2) compatible with

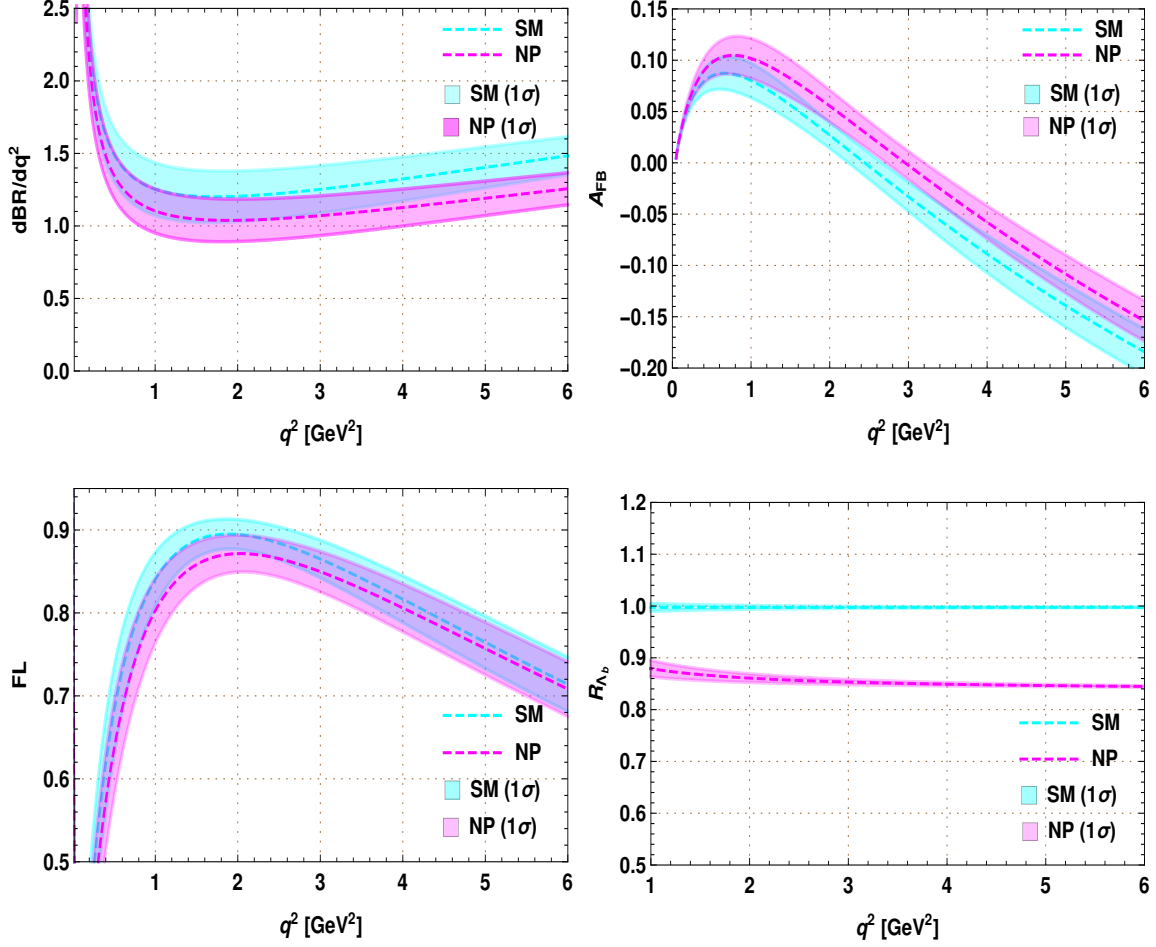


FIG. 6: The branching ratio (in units of 10^{-9}) (top left), forward backward asymmetry (top right), Polarisation asymmetry (bottom left) and R_{Λ_b} (bottom right) of $\Lambda_b \rightarrow \Lambda^*(1520)\mu^+\mu^-$ process.

LHCb experiment. The color description of the q^2 dependency and bin wise plots are as follows.

✎ **Distribution Plot:** The cyan dotted line represents the SM contribution, with the accompanying cyan band indicating the 1σ error band arising from uncertainties in the form factors and CKM elements. The magenta dotted line corresponds to the NP contribution, while the magenta band illustrates the 1σ uncertainty associated with this contribution.

✎ **Bin-wise Plot:** The SM and NP contributions are represented with crimson red and blue colors, respectively. .

Now, the detailed observations in the presence of NP contribution are provided as below.

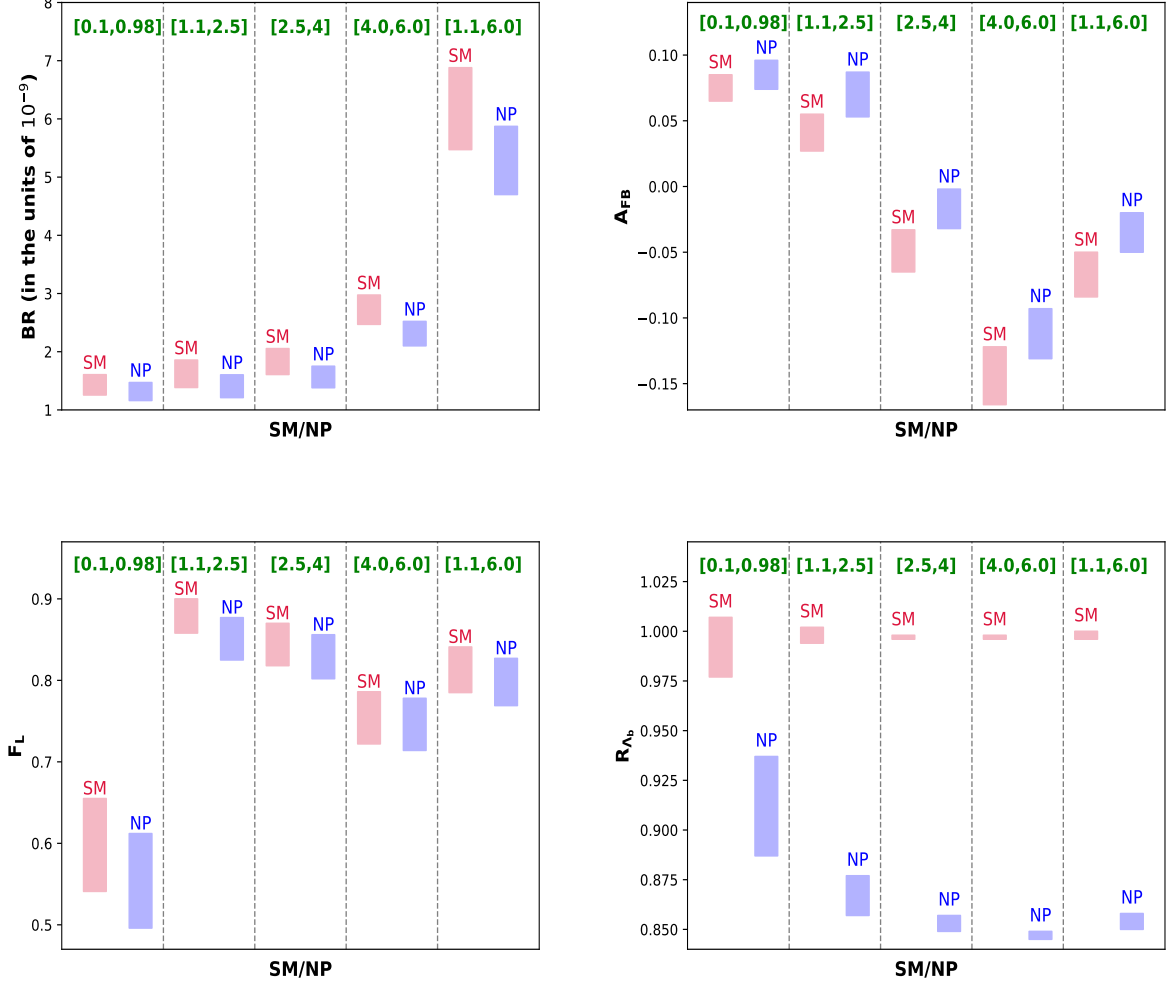


FIG. 7: BR (top left), A_{FB} (top right), F_L (bottom left) and R_{Λ_b} (bottom right) of $\Lambda_b \rightarrow \Lambda^*(1520)\mu^+\mu^-$ process are shown across q^2 bins: $q^2 \in [0.1, 0.98]$, $q^2 \in [1.1, 2.5]$, $q^2 \in [2.5, 4.0]$, $q^2 \in [4.0, 6.0]$, $q^2 \in [1.1, 6.0]$. The bands indicate 1σ uncertainty.

1. Branching ratio

The top-left panel of Fig. 6 illustrates the q^2 dependence of the branching ratio for the $\Lambda \rightarrow \Lambda^*(1520)(\rightarrow pK^-)\mu^+\mu^-$ decay, comparing the SM including new physics. In the presence of NP couplings, the branching ratio is found to be of the order $\mathcal{O}(10^{-9})$. The inclusion of the new vector coupling results in a reduction of $\text{BR}(\Lambda \rightarrow \Lambda^*(1520)(\rightarrow pK^-)\mu^+\mu^-)$, signifying a notable deviation from the SM prediction. The bin-wise plots are presented for both the SM and new physics in Fig. 7.

TABLE IV: Numerical predictions for branching ratio and other physical observables of $\Lambda_b \rightarrow \Lambda^*(1520)(\rightarrow pK^-)\ell^+\ell^-$ decay in SM and NP.

SM				
q^2 bin	$\langle BR \rangle_\mu \times 10^9$	$\langle R_{\Lambda_b} \rangle_{\mu/e}$	$\langle A_{FB} \rangle_\mu$	$\langle F_L \rangle_\mu$
[0.1, 0.98]	1.431 ± 0.175	0.992 ± 0.015	0.075 ± 0.010	0.598 ± 0.057
[1.1, 2.5]	1.621 ± 0.236	0.998 ± 0.004	0.041 ± 0.014	0.879 ± 0.021
[2.5, 4.0]	1.831 ± 0.223	0.997 ± 0.001	-0.049 ± 0.016	0.844 ± 0.026
[4.0, 6.0]	2.722 ± 0.252	0.997 ± 0.001	-0.144 ± 0.022	0.754 ± 0.032
[1.1, 6.0]	6.176 ± 0.704	0.998 ± 0.002	-0.067 ± 0.017	0.813 ± 0.028
NP				
q^2 bin	$\langle BR \rangle_\mu \times 10^9$	$\langle R_{\Lambda_b} \rangle_{\mu/e}$	$\langle A_{FB} \rangle_\mu$	$\langle F_L \rangle_\mu$
[0.1, 0.98]	1.316 ± 0.155	0.912 ± 0.025	0.085 ± 0.011	0.554 ± 0.058
[1.1, 2.5]	1.407 ± 0.196	0.867 ± 0.010	0.070 ± 0.017	0.851 ± 0.026
[2.5, 4.0]	1.566 ± 0.185	0.853 ± 0.004	-0.017 ± 0.015	0.829 ± 0.027
[4.0, 6.0]	2.311 ± 0.210	0.847 ± 0.002	-0.112 ± 0.019	0.746 ± 0.032
[1.1, 6.0]	5.286 ± 0.586	0.854 ± 0.004	-0.035 ± 0.015	0.798 ± 0.029

2. Longitudinal polarisation asymmetry

Due to the influence of the NP coupling, the contribution from new physics is shifted slightly lower compared to the SM. However, no significant deviation is observed for this particular observable. The corresponding q^2 -distribution and bin-wise plots are shown in the bottom-left panel of Fig. 6 and Fig. 7, respectively. In Table IV, we provide detailed numerical predictions for both the SM and new physics, offering a comprehensive comparison of theoretical expectations.

3. Forward-backward asymmetry

This observable exhibits a comparatively larger deviation compared to branching ratio and polarisation asymmetry. The q^2 distribution, illustrated in Fig. 6, reveals a zero-crossing point at approximately 2.5 GeV^2 in the SM. However, in the presence of new physics

couplings, the zero-crossing point shifts to around 3 GeV², a deviation that is distinctly noticeable compared to the Standard Model value at around 2.5 GeV².

4. *Lepton non-universal observable*

Notably, the ratio of branching ratios, specifically the LFU-sensitive observable R_{Λ_b} , reveals a profound distinction between the new physics contribution and the SM prediction. The NP contribution shows a marginal sensitivity, with the SM prediction being approximately 1. The q^2 -dependency and the bin-wise behavior are depicted in Fig. 6 and Fig. 7. Additionally, the predicted values in different bin ranges, computed using the benchmark values of the new coefficient, are presented in Table IV.

VII. CONCLUDING REMARKS

Motivated by the observed anomalies in $B \rightarrow (K, K^*)\mu^+\mu^-$ and $B_s \rightarrow \phi\mu^+\mu^-$ decays, which proceed via the $b \rightarrow s\mu^+\mu^-$ flavor-changing neutral current interaction, we examine the exclusive semileptonic $\Lambda \rightarrow \Lambda^*(1520)(\rightarrow pK^-)\mu^+\mu^-$ decay channel in the context of a $U(1)_{L_e-L_\mu}$ gauge extension. This extended model incorporates an enriched particle content, including three neutral fermions, the lightest of which contributes to the dark matter content of the Universe. Additionally, the scalar sector is augmented by a \tilde{R}_2 scalar leptoquark doublet to investigate flavor decays in the B -meson sector. Focusing on the muon mode in the final lepton pair, we constrain the NP coupling by considering the global analysis associated with observables of $B \rightarrow K^{(*)}\mu^+\mu^-$ and $B_s \rightarrow \phi\mu^+\mu^-$ decay channels. Furthermore the fermionic dark matter annihilates via scalar leptoquark components and Z' to provide the relic abundance of dark matter. DM-nucleon interaction gives spin-dependent cross section in leptoquark portal. Dark matter observables constrain the model parameters and the constrained parameter space is utilized in the flavor studies. Utilizing the allowed parameter space consistent with both flavor and dark matter sectors, we explore the impact on various observables, including the branching ratio, forward-backward asymmetry, polarization asymmetry, and lepton flavor universality violation in the $\Lambda_b \rightarrow \Lambda^*(1520)(\rightarrow pK)\ell^+\ell^-$ decay channel.

Our analysis reveals that the differential branching ratio is reduced compared to the SM,

indicating a significant deviation. We observe a substantial contribution from new physics in the analysis of the forward-backward asymmetry. The deviations detected in the lepton flavor universality observable R_{Λ_b} is clearly distinguishable, offering potential insights for future observations at the LHCb and Belle II experiments. It is crucial to gather more data from these experiments to fully understand the significance of the new physics contributions.

Acknowledgments

MKM acknowledges the financial support from IoE PDRF, University of Hyderabad. SS acknowledges the support of IoE project, University of Hyderabad and also IACS Kolkata institute funding for Research Associate-I. SS would like to thank Prof. Surov Roy for the hospitality provided in their research lab. DP extends appreciation for the support of Prime Minister's Research Fellowship, Government of India. RM would like to thank University of Hyderabad IoE project grant no. RC1-20-012. MKM extends sincere thanks to Dr. Suchismita Sahoo for the essential assistance in this work, also to Dr. Jacky Kumar and Dr. Girish Kumar for their valuable suggestions concerning the *flavio* package.

-
- [1] F. Zwicky, *Astrophys. J.* **86**, 217 (1937).
 - [2] V. C. Rubin and W. K. Ford, Jr., *Astrophys. J.* **159**, 379 (1970).
 - [3] D. Clowe, A. Gonzalez, and M. Markevitch, *Astrophys. J.* **604**, 596 (2004), [arXiv:astro-ph/0312273 \[astro-ph\]](#) .
 - [4] G. Bertone, D. Hooper, and J. Silk, *Phys. Rept.* **405**, 279 (2005), [arXiv:hep-ph/0404175](#) .
 - [5] N. Arkani-Hamed, D. P. Finkbeiner, T. R. Slatyer, and N. Weiner, *Phys. Rev. D* **79**, 015014 (2009), [arXiv:0810.0713 \[hep-ph\]](#) .
 - [6] S. Dodelson and L. M. Widrow, *Phys. Rev. Lett.* **72**, 17 (1994), [arXiv:hep-ph/9303287](#) .
 - [7] P. A. Zyla *et al.* (Particle Data Group), *PTEP* **2020**, 083C01 (2020).
 - [8] A. Sakharov, *Sov. Phys. Usp.* **34**, 392 (1991).
 - [9] E. W. Kolb and S. Wolfram, *Nucl. Phys. B* **172**, 224 (1980), [Erratum: *Nucl.Phys.B* 195, 542 (1982)].
 - [10] S. Davidson, E. Nardi, and Y. Nir, *Phys. Rept.* **466**, 105 (2008), [arXiv:0802.2962 \[hep-ph\]](#) .

- [11] W. Buchmuller, P. Di Bari, and M. Plumacher, *Annals Phys.* **315**, 305 (2005), [arXiv:hep-ph/0401240](#) .
- [12] A. Strumia, in *Les Houches Summer School on Theoretical Physics: Session 84: Particle Physics Beyond the Standard Model* (2006) pp. 655–680, [arXiv:hep-ph/0608347](#) .
- [13] G. Hiller and F. Kruger, *Phys. Rev. D* **69**, 074020 (2004), [arXiv:hep-ph/0310219](#) .
- [14] R. Aaij *et al.* (LHCb), *Phys. Rev. Lett.* **131**, 051803 (2023), [arXiv:2212.09152 \[hep-ex\]](#) .
- [15] R. Aaij *et al.* (LHCb), *Phys. Rev. D* **108**, 032002 (2023), [arXiv:2212.09153 \[hep-ex\]](#) .
- [16] R. Aaij *et al.* (LHCb), *Phys. Rev. Lett.* **111**, 191801 (2013), [arXiv:1308.1707 \[hep-ex\]](#) .
- [17] R. Aaij *et al.* (LHCb), *JHEP* **02**, 104 (2016), [arXiv:1512.04442 \[hep-ex\]](#) .
- [18] M. Aaboud *et al.* (ATLAS), *JHEP* **10**, 047 (2018), [arXiv:1805.04000 \[hep-ex\]](#) .
- [19] R. Aaij *et al.* (LHCb), *Phys. Rev. Lett.* **127**, 151801 (2021), [arXiv:2105.14007 \[hep-ex\]](#) .
- [20] R. Aaij *et al.* (LHCb), *JHEP* **09**, 179 (2015), [arXiv:1506.08777 \[hep-ex\]](#) .
- [21] R. Aaij *et al.* (LHCb), *Phys. Rev. Lett.* **128**, 191802 (2022), [arXiv:2110.09501 \[hep-ex\]](#) .
- [22] S. Singirala, S. Sahoo, and R. Mohanta, *Phys. Rev. D* **99**, 035042 (2019), [arXiv:1809.03213 \[hep-ph\]](#) .
- [23] S. Singirala, S. Sahoo, and R. Mohanta, *Phys. Rev. D* **105**, 015033 (2022), [arXiv:2106.03735 \[hep-ph\]](#) .
- [24] N. Rajeev and R. Dutta, *Phys. Rev. D* **105**, 115028 (2022), [arXiv:2112.11682 \[hep-ph\]](#) .
- [25] N. Rajeev, N. Sahoo, and R. Dutta, *Phys. Rev. D* **103**, 095007 (2021), [arXiv:2009.06213 \[hep-ph\]](#) .
- [26] N. Das and R. Dutta, *Phys. Rev. D* **108**, 095051 (2023), [arXiv:2307.03615 \[hep-ph\]](#) .
- [27] A. K. Yadav, M. K. Mohapatra, and S. Sahoo, in *22nd Conference on Flavor Physics and CP Violation* (2024) [arXiv:2408.16439 \[hep-ph\]](#) .
- [28] M. K. Mohapatra and A. Giri, *Phys. Rev. D* **104**, 095012 (2021), [arXiv:2109.12382 \[hep-ph\]](#) .
- [29] R. Dutta, *Phys. Rev. D* **100**, 075025 (2019), [arXiv:1906.02412 \[hep-ph\]](#) .
- [30] M. K. Mohapatra, N. Rajeev, and R. Dutta, *Phys. Rev. D* **105**, 115022 (2022), [arXiv:2108.10106 \[hep-ph\]](#) .
- [31] S. Sahoo and R. Mohanta, *New J. Phys.* **18**, 093051 (2016), [arXiv:1607.04449 \[hep-ph\]](#) .
- [32] C. Bobeth, A. J. Buras, F. Kruger, and J. Urban, *Nucl. Phys.* **B630**, 87 (2002), [arXiv:hep-ph/0112305 \[hep-ph\]](#) .
- [33] S. Descotes-Genon, S. Fajfer, J. F. Kamenik, and M. Novoa-Brunet, *Phys. Lett. B* **809**,

- 135769 (2020), [Addendum: Phys.Lett.B 840, 137830 (2023)], [arXiv:2005.03734 \[hep-ph\]](#) .
- [34] S. Fajfer, N. Košnik, and L. Vale Silva, *Eur. Phys. J. C* **78**, 275 (2018), [arXiv:1802.00786 \[hep-ph\]](#) .
- [35] M. K. Mohapatra, A. K. Yadav, and S. Sahoo, (2024), [arXiv:2409.01269 \[hep-ph\]](#) .
- [36] A. K. Yadav, M. K. Mohapatra, and S. Sahoo, (2024), [arXiv:2409.09737 \[hep-ph\]](#) .
- [37] M. Bauer and M. Neubert, *Phys. Rev. Lett.* **116**, 141802 (2016), [arXiv:1511.01900 \[hep-ph\]](#) .
- [38] D. Das, C. Hati, G. Kumar, and N. Mahajan, *Phys. Rev. D* **94**, 055034 (2016), [arXiv:1605.06313 \[hep-ph\]](#) .
- [39] D. Bečirević, S. Fajfer, N. Košnik, and O. Sumensari, *Phys. Rev. D* **94**, 115021 (2016), [arXiv:1608.08501 \[hep-ph\]](#) .
- [40] S. Sahoo, R. Mohanta, and A. K. Giri, *Phys. Rev. D* **95**, 035027 (2017), [arXiv:1609.04367 \[hep-ph\]](#) .
- [41] G. Hiller, D. Loose, and K. Schönwald, *JHEP* **12**, 027 (2016), [arXiv:1609.08895 \[hep-ph\]](#) .
- [42] A. Crivellin, G. D'Ambrosio, and J. Heeck, *Phys. Rev. D* **91**, 075006 (2015), [arXiv:1503.03477 \[hep-ph\]](#) .
- [43] P. Ko, Y. Omura, Y. Shigekami, and C. Yu, *Phys. Rev. D* **95**, 115040 (2017), [arXiv:1702.08666 \[hep-ph\]](#) .
- [44] S. F. King, *JHEP* **08**, 019 (2017), [arXiv:1706.06100 \[hep-ph\]](#) .
- [45] S. Di Chiara, A. Fowlie, S. Fraser, C. Marzo, L. Marzola, M. Raidal, and C. Spethmann, *Nucl. Phys. B* **923**, 245 (2017), [arXiv:1704.06200 \[hep-ph\]](#) .
- [46] R. Alonso, P. Cox, C. Han, and T. T. Yanagida, *Phys. Rev. D* **96**, 071701 (2017), [arXiv:1704.08158 \[hep-ph\]](#) .
- [47] C. Bonilla, T. Modak, R. Srivastava, and J. W. F. Valle, *Phys. Rev. D* **98**, 095002 (2018), [arXiv:1705.00915 \[hep-ph\]](#) .
- [48] J. Ellis, M. Fairbairn, and P. Tunney, *Eur. Phys. J. C* **78**, 238 (2018), [arXiv:1705.03447 \[hep-ph\]](#) .
- [49] R. Aaij *et al.* (LHCb), *Phys. Rev. Lett.* **115**, 072001 (2015), [arXiv:1507.03414 \[hep-ex\]](#) .
- [50] R. Aaij *et al.* (LHCb), *JHEP* **05**, 040 (2020), [arXiv:1912.08139 \[hep-ex\]](#) .
- [51] P. Agrawal, Z. Chacko, C. Kilic, and R. K. Mishra, (2010), [arXiv:1003.1912 \[hep-ph\]](#) .
- [52] A. V. Semenov, (1996), [arXiv:hep-ph/9608488 \[hep-ph\]](#) .
- [53] A. Pukhov, E. Boos, M. Dubinin, V. Edneral, V. Ilyin, D. Kovalenko, A. Kryukov, V. Savrin,

- S. Shichanin, and A. Semenov, (1999), [arXiv:hep-ph/9908288 \[hep-ph\]](#) .
- [54] G. Belanger, F. Boudjema, A. Pukhov, and A. Semenov, *Comput. Phys. Commun.* **176**, 367 (2007), [arXiv:hep-ph/0607059 \[hep-ph\]](#) .
- [55] G. Belanger, F. Boudjema, A. Pukhov, and A. Semenov, *Comput. Phys. Commun.* **180**, 747 (2009), [arXiv:0803.2360 \[hep-ph\]](#) .
- [56] C. Amole *et al.* (PICO), *Phys. Rev. D* **100**, 022001 (2019), [arXiv:1902.04031 \[astro-ph.CO\]](#) .
- [57] N. Aghanim *et al.* (Planck), (2018), [arXiv:1807.06209 \[astro-ph.CO\]](#) .
- [58] E. Ma, *Phys. Rev. D* **73**, 077301 (2006), [arXiv:hep-ph/0601225 \[hep-ph\]](#) .
- [59] A. Vicente, (2015), [arXiv:1507.06349 \[hep-ph\]](#) .
- [60] C. Bobeth, M. Misiak, and J. Urban, *Nucl. Phys. B* **574**, 291 (2000), [arXiv:hep-ph/9910220 \[hep-ph\]](#) .
- [61] A. J. Buras and M. Munz, *Phys. Rev. D* **52**, 186 (1995), [arXiv:hep-ph/9501281](#) .
- [62] R. Aaij *et al.* (LHCb), *JHEP* **06**, 133 (2014), [arXiv:1403.8044 \[hep-ex\]](#) .
- [63] R. Aaij *et al.* (LHCb), *JHEP* **11**, 047 (2016), [Erratum: *JHEP* 04, 142 (2017)], [arXiv:1606.04731 \[hep-ex\]](#) .
- [64] R. Aaij *et al.* (LHCb), *Phys. Rev. Lett.* **125**, 011802 (2020), [arXiv:2003.04831 \[hep-ex\]](#) .
- [65] R. Aaij *et al.* (LHCb), *Phys. Rev. Lett.* **126**, 161802 (2021), [arXiv:2012.13241 \[hep-ex\]](#) .
- [66] D. M. Straub, (2018), [arXiv:1810.08132 \[hep-ph\]](#) .
- [67] S. Navas *et al.* (Particle Data Group), *Phys. Rev. D* **110**, 030001 (2024).
- [68] S. Descotes-Genon and M. Novoa-Brunet, *JHEP* **06**, 136 (2019), [Erratum: *JHEP* 06, 102 (2020)], [arXiv:1903.00448 \[hep-ph\]](#) .
- [69] D. Das and J. Das, *JHEP* **07**, 002 (2020), [arXiv:2003.08366 \[hep-ph\]](#) .
- [70] Y.-S. Li, S.-P. Jin, J. Gao, and X. Liu, *Phys. Rev. D* **107**, 093003 (2023), [arXiv:2210.04640 \[hep-ph\]](#) .